Chapter 3

Discrete time dynamics

> Do it again!
> —Isabelle, age 3

(R. Mainieri and P. Cvitanović)

T HE TIME PARAMETER in the sect. 2.1 definition of a dynamical system can be either continuous or discrete. Discrete time dynamical systems arise naturally from flows; one can observe the flow at fixed time intervals (by strobing it), or one can record the coordinates of the flow when a special event happens (the Poincaré section method). This triggering event can be as simple as vanishing of one of the coordinates, or as complicated as the flow cutting through a curved hypersurface.

3.1 Poincaré sections

Successive trajectory intersections with a *Poincaré section*, a $(d-1)$-dimensional hypersurface or a set of hypersurfaces $\mathcal{P}$ embedded in the d-dimensional state space $\mathcal{M}$, define the *Poincaré return map* $P(x)$, a $(d-1)$-dimensional map of form

$$x' = P(x) = f^{\tau(x)}(x), \qquad x', x \in \mathcal{P}. \tag{3.1}$$

Here the *first return function* $\tau(x)$–sometimes referred to as the *ceiling function*–is the time of flight to the next section for a trajectory starting at x. The choice of the section hypersurface $\mathcal{P}$ is altogether arbitrary. It is rarely possible to define a single section that cuts across all trajectories of interest. In practice one often needs only a local section–a finite hypersurface of codimension 1 volume intersected by a ray of trajectories near to the trajectory of interest. The hypersurface can be specified implicitly through a function $U(x)$ that is zero whenever a point x is on the Poincaré section,

$$x \in \mathcal{P} \quad \text{iff} \quad U(x) = 0. \tag{3.2}$$

Figure 3.1: A $x(t)$ trajectory that intersects a Poincaré section $\mathcal{P}$ at times t_1, t_2, t_3, t_4, and closes a cycle (x_1, x_2, x_3, x_4), $x_k = x(t_k) \in \mathcal{P}$ of topological length 4 with respect to this section. Note that the intersections are not normal to the section, and that the crossing z does not count, as it in the wrong direction.
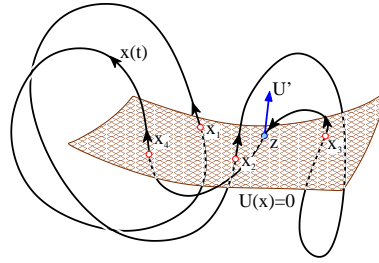
The gradient of $U(x)$ evaluated at $x \in \mathcal{P}$ serves a two-fold function. First, the flow should pierce the hypersurface $\mathcal{P}$, rather than being tangent to it. A nearby point $x + \delta x$ is in the hypersurface $\mathcal{P}$ if $U(x + \delta x) = 0$. A nearby point on the trajectory is given by $\delta x = v \delta t$, so a traversal is ensured by the *transversality condition*

$$(v \cdot \partial U) = \sum_{j=1}^{d} v_j(x)\partial_j U(x) \neq 0, \quad \partial_j U(x) = \frac{d}{dx_j}U(x), \quad x \in \mathcal{P}. \qquad (3.3)$$

Second, the gradient $\partial_j U$ defines the orientation of the hypersurface $\mathcal{P}$. The flow is oriented as well, and a periodic orbit can pierce $\mathcal{P}$ twice, traversing it in either direction, as in figure 3.1. Hence the definition of Poincaré return map $P(x)$ needs to be supplemented with the orientation condition

$$x_{n+1} = P(x_n), \qquad U(x_{n+1}) = U(x_n) = 0, \quad n \in \mathbb{Z}^+$$

$$\sum_{j=1}^{d} v_j(x_n)\partial_j U(x_n) > 0. \qquad (3.4)$$

In this way the continuous time t flow $f^t(x)$ is reduced to a discrete time n sequence x_n of successive *oriented* trajectory traversals of $\mathcal{P}$.

[chapter 15]

With a sufficiently clever choice of a Poincaré section or a set of sections, any orbit of interest intersects a section. Depending on the application, one might need to convert the discrete time n back to the continuous flow time. This is accomplished by adding up the first return function times $\tau(x_n)$, with the accumulated flight time given by

$$t_{n+1} = t_n + \tau(x_n), \qquad t_0 = 0, \qquad x_n \in \mathcal{P}. \qquad (3.5)$$

Other quantities integrated along the trajectory can be defined in a similar manner, and will need to be evaluated in the process of evaluating dynamical averages.

A few examples may help visualize this.

Example 3.1 Hyperplane $\mathcal{P}$: *The simplest choice of a Poincaré section is a plane $\mathcal{P}$ specified by a point (located at the tip of the vector r_0) and a direction vector a perpendicular to the plane. A point x is in this plane if it satisfies the condition*

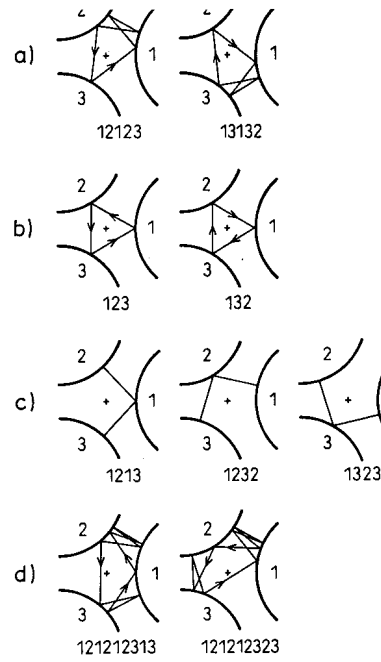$$U(x) = (x - r_0) \cdot a = 0. \qquad (3.6)$$

Figure 3.2: Some examples of 3-disk cycles: (a) $\overline{12123}$ and $\overline{13132}$ are mapped into each other by the flip across 1 axis. Similarly (b) $\overline{123}$ and $\overline{132}$ are related by flips, and (c) $\overline{1213}$, $\overline{1232}$ and $\overline{1323}$ by rotations. (d) The cycles $\overline{121212313}$ and $\overline{121212323}$ are related by rotation *and* time reversal. These symmetries are discussed in chapter 9. (From ref. [7])

Consider a circular periodic orbit centered at r_0, but not lying in $\mathcal{P}$. It pierces the hyperplane twice; the $(v \cdot a) > 0$ traversal orientation condition (3.4) ensures that the first return time is the full period of the cycle.

The above flat hyperplane is an *ad hoc* construct; one Poincaré section rarely suffices to capture all of the dynamics of interest. A more insightful picture of the dynamics is obtained by partitioning the state space into N qualitatively distinct regions $\{\mathcal{M}_1, \mathcal{M}_2, \ldots, \mathcal{M}_N\}$ and constructing a Poincaré section $\mathcal{P}_s$ per region. The d-dimensional flow is thus reduced reduced to composition

[section 10.1]

$$P_{s_n \leftarrow s_{n-1}} \circ \cdots \circ P_{s_2 \leftarrow s_1} \circ P_{s_1 \leftarrow s_0}$$

of a set of $(d-1)$-dimensional maps

$$P_{s_{n+1} \leftarrow s_n} : \quad x_n \mapsto x_{n+1}, \qquad s \in \{1, 2, \ldots, N\} \tag{3.7}$$

that map the coordinates of Poincaré section $\mathcal{P}_{s_n}$ to those of $\mathcal{P}_{s_{n+1}}$, the next section traversed by a given trajectory.

A *return map* P_{s_0} from section $\mathcal{P}_{s_0}$ to itself now has a contribution from any admissible (i.e., there exist trajectories that traverse regions $\mathcal{M}_{s_0} \to \mathcal{M}_{s_1} \to \cdots \to \mathcal{M}_{s_n} \to \mathcal{M}_{s_0}$ in the same temporal sequence) periodic sequence of compositions

$$P_{s_0 s_1 \cdots s_{n-1}} = P_{s_0 \leftarrow s_{n-1}} \circ \cdots \circ P_{s_2 \leftarrow s_1} \circ P_{s_1 \leftarrow s_0} \tag{3.8}$$

The next example   offers an unambiguous set of such Poincaré sections which do double duty, providing us both with an exact representation of dynamics in terms of maps, and with a covering symbolic dynamics, a subject that will will return to in chapter 10.
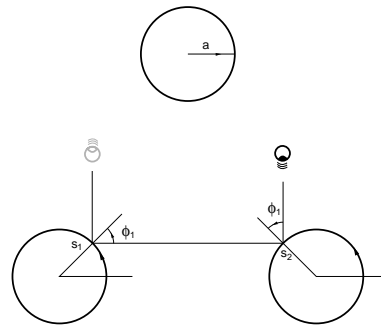
[chapter 10]

Figure 3.3: Poincaré section coordinates for the 3-disk game of pinball.
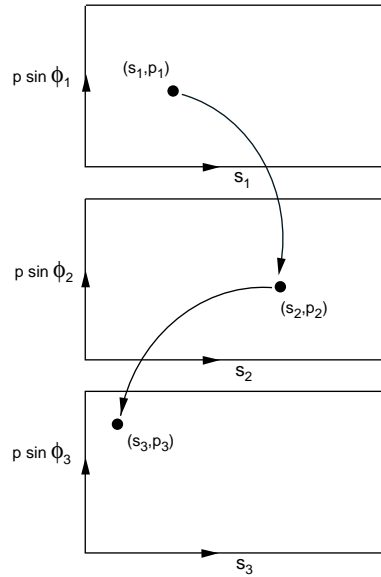

Figure 3.4: Collision sequence $(s_1, p_1) \mapsto (s_2, p_2) \mapsto (s_3, p_3)$ from the boundary of a disk to the boundary of the next disk is coded by the Poincaré sections maps sequence $P_{3\leftarrow2}P_{2\leftarrow1}$.

Example 3.2 *Pinball game, Poincaré dissected.* *A phase space orbit is fully specified by its position and momentum at a given instant, so no two distinct phase space trajectories can intersect. The configuration space trajectories, however, can and do intersect, in rather unilluminating ways, as e.g. in figure 3.2 (d), and it can be rather hard to perceive the systematics of orbits from their configuration space shapes. The problem is that we are looking at the projections of a 4-dimensional state space trajectories onto a 2-dimensional configuration subspace. A much clearer picture of the dynamics is obtained by constructing a set of state space Poincaré sections.*

Suppose that the pinball has just bounced off disk 1. Depending on its position and outgoing angle, it could proceed to either disk 2 or 3. Not much happens in between the bounces–the ball just travels at constant velocity along a straight line– so we can reduce the 4-dimensional flow to a 2-dimensional map $P_{\sigma_k \leftarrow \sigma_j}$ that maps the coordinates (Poincaré section $\mathcal{P}_1$) of the pinball from one disk edge to another. Just after the moment of impact the trajectory is defined by s_n, the arc-length position of the nth bounce along the billiard wall, and $p_n = p \sin \phi_n$ the momentum component parallel to the billiard wall at the point of impact, figure 3.3. These coordinates (due to Birkhoff) are smart, as they conserve the phase space volume. Trajectories originating from one disk can hit either of the other two disks, or escape without further ado. We label the survivor state space regions $\mathcal{P}_{12}, \mathcal{P}_{13}$. In terms of the three Poincaré sections, one for each disk, the dynamics is reduced to the set of six maps

$$P_{\sigma_{n+1} \leftarrow \sigma_n} : \quad (s_n, p_n) \mapsto (s_{n+1}, p_{n+1}), \qquad \sigma \in \{1, 2, 3\} \tag{3.9}$$

from the boundary of the disk j to the boundary of the next disk k, figure 3.4. The explicit form of this map is easily written down, see sect. 8, but much more economical
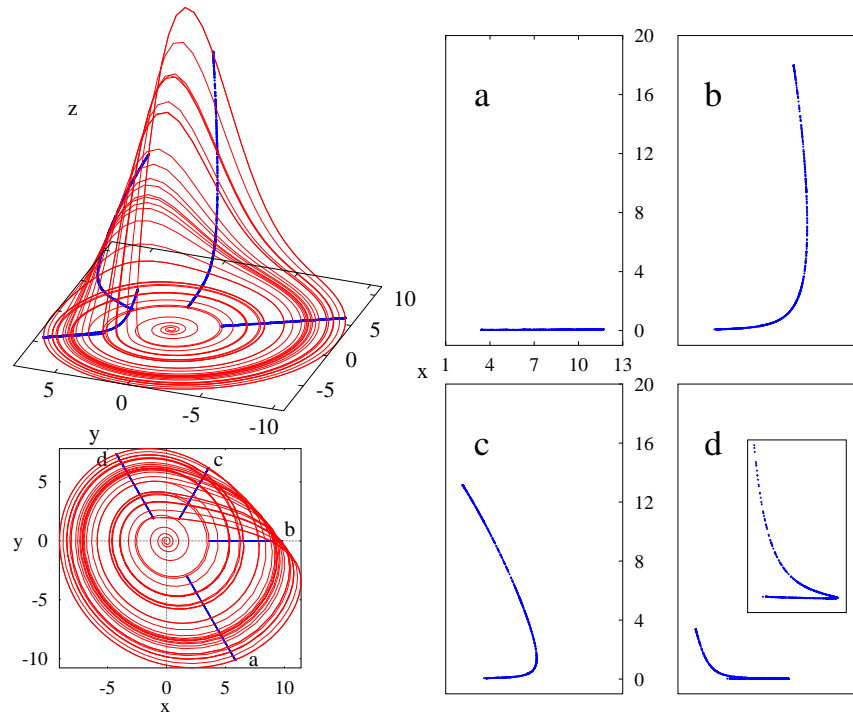
Figure 3.5: (Right:) a sequence of Poincaré sections of the Rössler strange attractor, defined by planes through the z axis, oriented at angles (a) -60° (b) 0°, (c) 60°, (d) 120°, in the x-y plane. (Left:) side and x-y plane view of a typical trajectory with Poincaré sections superimposed. (R. Paškauskas)

is the symmetry quotiented version of chapter 9 which replaces the above 6 maps by a return map pair P_0, P_1.

[chapter 9]

[chapter 8]

Embedded within $\mathcal{P}_{12}, \mathcal{P}_{13}$ are four strips $\mathcal{P}_{121}, \mathcal{P}_{123}, \mathcal{P}_{131}, \mathcal{P}_{132}$ of initial conditions that survive two bounces, and so forth. Provided that the disks are sufficiently separated, after n bounces the survivors are labeled by 2^n distinct itineraries $\sigma_1\sigma_2\sigma_3 \ldots \sigma_n$.

Billiard dynamics is exceptionally simple - free flight segments, followed by specular reflections at boundaries, thus billiard boundaries are the obvious choice as Poincaré sections. What about smooth, continuous time flows, with no obvious surfaces that would fix the choice of Poincaré sections?

Example 3.3 Pendulum: The phase space of a simple pendulum is 2-dimensional: momentum on the vertical axis and position on the horizontal axis. We choose the Poincaré section to be the positive horizontal axis. Now imagine what happens as a point traces a trajectory through this phase space. As long as the motion is oscillatory, in the pendulum all orbits are loops, so any trajectory will periodically intersect the line, that is the Poincaré section, at one point.

Consider next a pendulum with friction, such as the unforced Duffing system plotted in figure 2.3. Now every trajectory is an inward spiral, and the trajectory will intersect the Poincaré section $y = 0$ at a series of points that get closer and closer to either of the equilibrium points; the Duffing oscillator at rest.

Motion of a pendulum is so simple that you can sketch it yourself on a piece of paper. The next example offers a better illustration of the utility of visualization of dynamics by means of Poincaré sections.

Example 3.4 Rössler flow: Consider figure 2.5, a typical trajectory of the 3-dimensional Rössler flow (2.17). It wraps around the z axis, so a good choice for a

Figure 3.6: Return maps for the $R_n \rightarrow R_{n+1}$ radial distance Poincaré sections of figure 3.5. (R. Paškauskas)
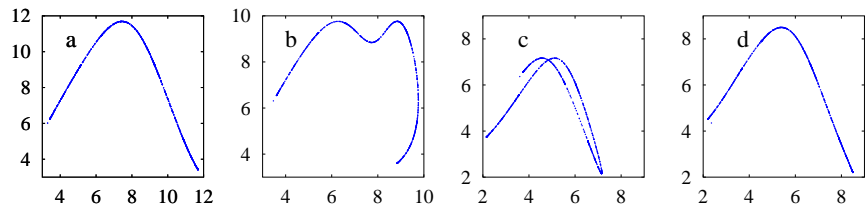
Poincaré section is a plane passing through the z axis. A sequence of such Poincaré sections placed radially at increasing angles with respect to the x axis, figure 3.5, illustrates the "stretch & fold" action of the Rössler flow. To orient yourself, compare this with figure 2.5, and note the different z-axis scales. Figure 3.5 assembles these sections into a series of snapshots of the flow. A line segment $[A, B]$, traversing the width of the attractor, starts out close to the x-y plane, and after the stretching (a) $\rightarrow$ (b) followed by the folding (c) $\rightarrow$ (d), the folded segment returns close to the x-y plane strongly compressed. In one Poincaré return the $[A, B]$ interval is stretched, folded and mapped onto itself, so the flow is expanding. *It is also* mixing, *as in one Poincaré return the point C from the interior of the attractor is mapped into the outer edge, while the edge point B lands in the interior.*

Once a particular Poincaré section is picked, we can also exhibit the return map (3.1), as in figure 3.6. Cases (a) and (d) are examples of nice 1-to-1 return maps. However, (b) and (c) appear multimodal and non-invertible, artifacts of projection of a 2-d return map $(R_n, z_n) \rightarrow (R_{n+1}, z_{n+1})$ onto a 1-dimensional subspace $R_n \rightarrow R_{n+1}$. (Continued in example 4.1)

fast track:
sect. 3.3, p. 54

The above examples illustrate why a Poincaré section gives a more informative snapshot of the flow than the full flow portrait. For example, while the full flow portrait of the Rössler flow figure 2.5 gives us no sense of the thickness of the attractor, we see clearly in the figure 3.5 Poincaré sections that even though the return map is 2-d $\rightarrow$ 2-d, the flow contraction is so strong that for all practical purposes it renders the return map 1-dimensional.

### 3.1.1 What's the best Poincaré section?

In practice, picking sections is a dark and painful art, especially for high-dimensional flows where the human visual cortex falls short. It helps to understand why we need them in the first place.

Whenever a system has a continuous symmetry G, any two solutions related by the symmetry are equivalent, so it would be stupid to keep recomputing them over and over. We would rather replace the whole continuous family of solutions by one.

A smart way to do would be to replace dynamics $(\mathcal{M}, f)$ by dynamics on the *quotient state space* $(\mathcal{M}/G, \tilde{f})$. We will discuss this in chapter 9, but in general constructing explicit quotient state space flow $\tilde{f}$ appears either difficult, or not

[chapter 9]

Figure 3.7: (a) Lorenz flow figure 2.4 cut by $y = x$ Poincaré section plane $\mathcal{P}$ through the z axis and both $EQ_{1,2}$ equilibria. Points where flow pierces into section are marked by dots. To aid visualization of the flow near the EQ_0 equilibrium, the flow is cut by the second Poincaré section, $\mathcal{P}'$, through $y = -x$ and the z axis. (b) Poincaré sections $\mathcal{P}$ and $\mathcal{P}'$ laid side-by-side. The singular nature of these sections close to EQ_0 will be elucidated in example 4.6 and figure 10.7 (b). (E. Siminos)
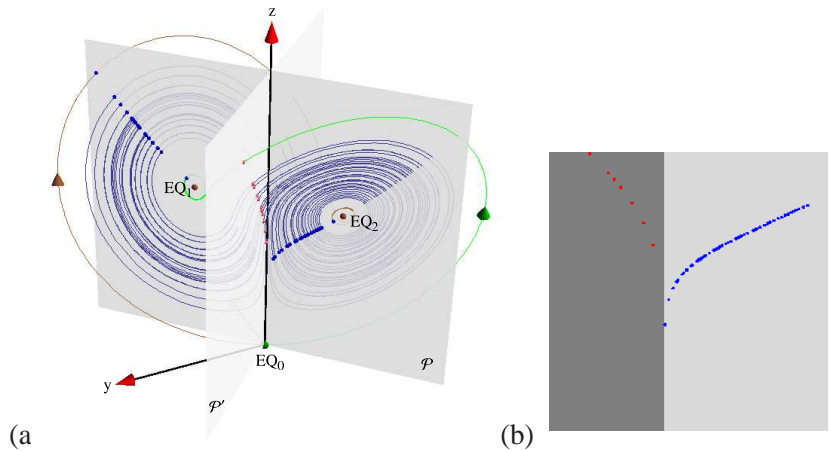
appreciated enough to generate much readable literature, or perhaps impossible. So one resorts to method of sections.

Time evolution itself is a 1-parameter abelian Lie group, albeit a highly nontrivial one (otherwise this book would not be much of a doorstop). The invariants of the flow are its infinite-time orbits; particularly useful invariants are compact orbits $\mathcal{M}_p \subset \mathcal{M}$, such as equilibrium points, periodic orbits and tori. For any orbit it suffices to pick a single state space point $x \in \mathcal{M}_p$, the rest of the orbit is generated by the flow and its symmetries.

Choice of this one point is utterly arbitrary; in dynamics this is called a "Poincaré section," and in theoretical physics this goes by the exceptionally uninformative name of "gauge fixing." The price is that one generates "ghosts," or, in dynamics, increases the dimensionality of the state space by additional constraints (see sect. 12.4). It is a commonly deployed but inelegant procedure where symmetry is broken for computational convenience, and restored only at the end of the calculation, when all broken pieces are reassembled.

This said, there are a few rules of thumb to follow: (a) You can pick as many sections as convenient. (b) For ease of computation, pick linear sections (3.6) if you can. (c) If equilibria play important role in organizing a flow, pick sections that go through them (see example 3.5). (c) If you have a global discrete or continuous symmetry, pick sections left invariant by the symmetry (see example 9.2). [chapter 9] (d) If you are solving a local problem, like finding a periodic orbit, you do not need a global section. Pick a section or a set of (multi-shooting) sections on the fly, requiring only that they are locally orthogonal to the flow (e) If you have another rule of thumb dear to you, let us know.

Example 3.5 *Sections of Lorenz flow:* *(Continued from example 2.2.) The plane $\mathcal{P}$ fixed by the $x = y$ diagonal and the z-axis depicted in figure 3.7 is a natural choice of a Poincaré section of the Lorenz flow of figure 2.4, as it contains all three equilibria, $x_{EQ0} = (0,0,0)$ and the (2.13) pair $EQ_{1,2}$. A section has to be supplemented with the orientation condition (3.4): here points where flow pierces into the section are marked by dots.*

$EQ_{1,2}$ are centers of out-spirals, and close to them the section is transverse to the flow. However, close to EQ_0 trajectories pass the z-axis either by crossing the

section $\mathcal{P}$ or staying on the viewer's side. We are free to deploy as many sections as we wish: in order to capture the whole flow in this neighborhood we add the second Poincaré section, $\mathcal{P}'$, through the $y = -x$ diagonal and the z-axis. Together the two sections, figure 3.7 (b), capture the whole flow near EQ_0. In contrast to Rössler sections of figure 3.5, these appear very singular. We explain this singularity in example 4.6, and postpone construction of a Poincaré return map to example 9.2.

(E. Siminos and J. Halcrow)

3.2 Constructing a Poincaré section

For almost any flow of physical interest a Poincaré section is not available in analytic form. We describe now a numerical method for determining a Poincaré section.

[remark 3.1]

Consider the system (2.6) of ordinary differential equations in the vector variable $x = (x_1, x_2, \ldots, x_d)$

$$\frac{dx_i}{dt} = v_i(x, t), \tag{3.10}$$

where the flow velocity v is a vector function of the position in state space x and the time t. In general, v cannot be integrated analytically, so we will have to resort to numerical integration to determine the trajectories of the system. Our task is to determine the points at which the numerically integrated trajectory traverses a given hypersurface. The hypersurface will be specified implicitly through a function $U(x)$ that is zero whenever a point x is on the Poincaré section, such as the hyperplane (3.6).

If we use a tiny step size in our numerical integrator, we can observe the value of U as we integrate; its sign will change as the trajectory crosses the hypersurface. The problem with this method is that we have to use a very small integration time step. In order to land exactly on the Poincaré section one often interpolates the intersection point from the two trajectory points on either side of the hypersurface. However, there is a better way.

Let t_a be the time just before U changes sign, and t_b the time just after it changes sign. The method for landing exactly on the Poincaré section will be to convert one of the space coordinates into an integration variable for the part of the trajectory between t_a and t_b. Using

$$\frac{dx_k}{dx_1}\frac{dx_1}{dt} = \frac{dx_k}{dx_1}v_1(x, t) = v_k(x, t) \tag{3.11}$$

we can rewrite the equations of motion (3.10) as

$$\frac{dt}{dx_1} = \frac{1}{v_1}, \quad \cdots, \quad \frac{dx_d}{dx_1} = \frac{v_d}{v_1}. \tag{3.12}$$

Now we use x_1 as the 'time' in the integration routine and integrate it from $x_1(t_a)$ to the value of x_1 on the hypersurface, determined by the hypersurface intersection condition (3.6). This is the end point of the integration, with no need for any interpolation or backtracking to the surface of section. The x_1–axis need not be perpendicular to the Poincaré section; any x_i can be chosen as the integration variable, provided the x_i-axis is not parallel to the Poincaré section at the trajectory intersection point. If the section crossing is transverse (3.3), v_1 cannot vanish in the short segment bracketed by the integration step preceding the section, and the point on the Poincaré section.

Example 3.6 *Computation of Rössler flow Poincaré sections.* *Poincaré sections of figure 3.5 are defined by the fixing angle $U(x) = \theta - \theta_0 = 0$. Convert Rössler equation (2.17) to cylindrical coordinates:*

$$\begin{aligned} \dot{r} &= v_r = -z\cos\theta + ar\sin^2\theta \\ \dot{\theta} &= v_\theta = 1 + \frac{z}{r}\sin\theta + \frac{a}{2}\sin 2\theta \\ \dot{z} &= v_z = b + z(r\cos\theta - c)\,. \end{aligned} \qquad (3.13)$$

In principle one should use the equilibrium x_+ from (2.18) as the origin, and its eigenvectors as the coordinate frame, but here original coordinates suffice, as for parameter values (2.17), and (x_0, y_0, z_0) sufficiently far away from the inner equilibrium, θ increases monotonically with time. Integrate

$$\frac{dr}{d\theta} = v_r/v_\theta\,, \quad \frac{dt}{d\theta} = 1/v_\theta\,, \quad \frac{dz}{d\theta} = v_z/v_\theta \qquad (3.14)$$

from (r_n, θ_n, z_n) to the next Poincaré section at θ_{n+1}, and switch the integration back to (x, y, z) coordinates.   *(Radford Mitchell, Jr.)*

3.3   Maps

Though we have motivated discrete time dynamics by considering sections of a continuous flow, there are many settings in which dynamics is inherently discrete, and naturally described by repeated iterations of the same map

$$f : \mathcal{M} \to \mathcal{M}\,,$$

or sequences of consecutive applications of a finite set of maps,

$$\{f_A, f_B, \dots f_Z\} : \mathcal{M} \to \mathcal{M}\,, \qquad (3.15)$$

for example maps relating different sections among a set of Poincaré sections. The discrete 'time' is then an integer, the number of applications of a map. As writing out formulas involving repeated applications of a set of maps explicitly can be awkward, we streamline the notation by denoting a map composition by '$\circ$'

$$f_Z(\cdots f_B(f_A(x)))\cdots) = f_Z \circ \cdots f_B \circ f_A(x)\,, \qquad (3.16)$$

Figure 3.8: A flow $x(t)$ of figure 3.1 represented by a Poincaré return map that maps points in the Poincaré section $\mathcal{P}$ as $x_{n+1} = f(x_n)$. In this example the orbit of x_1 consists of the four cycle points (x_1, x_2, x_3, x_4)
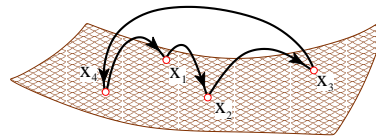
and the nth iterate of map f by

$$f^n(x) = f \circ f^{n-1}(x) = f\left(f^{n-1}(x)\right), \qquad f^0(x) = x.$$

The *trajectory* of x is now the discrete set of points

$$\left\{x, f(x), f^2(x), \dots, f^n(x)\right\},$$

and the *orbit* of x is the subset of all points of $\mathcal{M}$ that can be reached by iterations of f. For example, the orbit of x_1 in figure 3.8 is the 4-cycle (x_1, x_2, x_3, x_4).

The functional form of such Poincaré return maps P as figure 3.6 can be approximated by tabulating the results of integration of the flow from x to the first Poincaré section return for many $x \in \mathcal{P}$, and constructing a function that interpolates through these points. If we find a good approximation to $P(x)$, we can get rid of numerical integration altogether, by replacing the continuous time trajectory $f^t(x)$ by iteration of the Poincaré return map $P(x)$. Constructing accurate $P(x)$ for a given flow can be tricky, but we can already learn much from approximate Poincaré return maps. Multinomial approximations

$$P_k(x) = a_k + \sum_{j=1}^{d} b_{kj}x_j + \sum_{i,j=1}^{d} c_{kij}x_ix_j + \dots, \qquad x \in \mathcal{P} \tag{3.17}$$

to Poincaré return maps

$$\begin{pmatrix} x_{1,n+1} \\ x_{2,n+1} \\ \dots \\ x_{d,n+1} \end{pmatrix} = \begin{pmatrix} P_1(x_n) \\ P_2(x_n) \\ \dots \\ P_d(x_n) \end{pmatrix}, \qquad x_n, x_{n+1} \in \mathcal{P}$$

motivate the study of model mappings of the plane, such as the Hénon map.

Example 3.7 *Hénon map:* *The map*

$$\begin{aligned} x_{n+1} &= 1 - ax_n^2 + by_n \\ y_{n+1} &= x_n \end{aligned} \tag{3.18}$$

is a nonlinear 2-dimensional map most frequently employed in testing various hunches about chaotic dynamics. The Hénon map is sometimes written as a 2-step recurrence relation

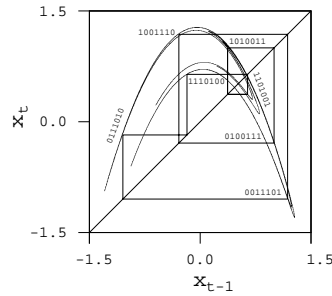$$x_{n+1} = 1 - ax_n^2 + bx_{n-1}. \tag{3.19}$$

Figure 3.9: The strange attractor and an unstable period 7 cycle of the Hénon map (3.18) with $a = 1.4$, $b = 0.3$. The periodic points in the cycle are connected to guide the eye. (K.T. Hansen [8])

An n-step recurrence relation is the discrete-time analogue of an nth order differential equation, and it can always be replaced by a set of n 1-step recurrence relations.

The Hénon map is the simplest map that captures the "stretch & fold" dynamics of return maps such as Rössler's, figure 3.5. It can be obtained by a truncation of a polynomial approximation (3.17) to a Poincaré return map (3.17) to second order.

A quick sketch of the long-time dynamics of such a mapping (an example is depicted in figure 3.9), is obtained by picking an arbitrary starting point and iterating (3.18) on a computer. We plot here the dynamics in the (x_n, x_{n+1}) plane, rather than in the (x_n, y_n) plane, because we think of the Hénon map as a model return map $x_n \to x_{n+1}$. As we shall soon see, periodic orbits will be key to understanding the long-time dynamics, so we also plot a typical periodic orbit of such a system, in this case an unstable period 7 cycle. Numerical determination of such cycles will be explained in sect. 27.1 , and the cycle point labels $0111010, 1110100, \cdots$ in sect. 11.3.

[exercise 3.5]

Example 3.8 *Lozi map:* *Another example frequently employed is the* Lozi map*, a linear, 'tent map' version of the Hénon map (3.18) given by*

$$\begin{aligned} x_{n+1} &= 1 - a|x_n| + by_n \\ y_{n+1} &= x_n\,. \end{aligned} \qquad (3.20)$$

Though not realistic as an approximation to a smooth flow, the Lozi map is a very helpful tool for developing intuition about the topology of a large class of maps of the "stretch & fold" type.

What we get by iterating such maps is–at least qualitatively–not unlike what we get from Poincaré section of flows such as the Rössler flow figure 3.6. For an arbitrary initial point this process might converge to a stable limit cycle, to a strange attractor, to a false attractor (due to roundoff errors), or diverge. In other words, mindless iteration is essentially uncontrollable, and we will need to resort to more thoughtful explorations. As we shall explain in due course, strategies for systematic exploration rely on stable/unstable manifolds, periodic points, saddle-straddle methods and so on.

[exercise 3.5]

Example 3.9 *Parabola:* *For sufficiently large value of the stretching paramater a, one iteration of the Hénon map (3.18) stretches and folds a region of the (x, y) plane centered around the origin. The parameter a controls the amount of stretching, while*

the parameter b controls the thickness of the folded image through the '1-step memory' term bx_{n-1} in (3.19). In figure 3.9 the parameter b is rather large, $b = 0.3$, so the attractor is rather thick, with the transverse fractal structure clearly visible. For vanishingly small b the Hénon map reduces to the 1-dimensional quadratic map

$$x_{n+1} = 1 - ax_n^2.\qquad\qquad(3.21)$$

[exercise 3.7]

By setting $b = 0$ we lose determinism, as on reals the inverse of map (3.21) has two preimages $\{x_{n-1}^+, x_{n-1}^-\}$ for most x_n. If Bourbaki is your native dialect: the Hénon map is injective *or one-to-one, but the quadratic map is* surjective *or many-to-one. Still, this 1-dimensional approximation is very instructive.*

As we shall see in sect. 10.2.1, an understanding of 1-dimensional dynamics is indeed the essential prerequisite to unraveling the qualitative dynamics of many higher-dimensional dynamical systems. For this reason many expositions of the theory of dynamical systems commence with a study of 1-dimensional maps. We prefer to stick to flows, as that is where the physics is.

[appendix H.8]

Résumé

In recurrent dynamics a trajectory exits a region in state space and then reenters it infinitely often, with a finite mean return time. If the orbit is periodic, it returns after a full period. So, on average, nothing much really happens along the trajectory–what is important is behavior of neighboring trajectories transverse to the flow. This observation motivates a replacement of the continuous time flow by iterative mapping, the Poincaré return map.

The visualization of strange attractors is greatly facilitated by a felicitous choice of Poincaré sections, and the reduction of flows to Poincaré return maps. This observation motivates in turn the study of discrete-time dynamical systems generated by iterations of maps.

A particularly natural application of the Poincaré section method is the reduction of a billiard flow to a boundary-to-boundary return map, described in chapter 8. As we shall show in chapter 6, further simplification of a Poincaré return map, or any nonlinear map, can be attained through rectifying these maps locally by means of smooth conjugacies.

[chapter 8]
[chapter 6]

Commentary

Remark 3.1 Determining a Poincaré section. The idea of changing the integration variable from time to one of the coordinates, although simple, avoids the alternative of having to interpolate the numerical solution to determine the intersection. The trick described in sect. 3.2 is due to Hénon [5, 6, 7].

Remark 3.2 Hénon, Lozi maps. The Hénon map is of no particular physical import in and of itself–its significance lies in the fact that it is a minimal normal form for modeling flows near a saddle-node bifurcation, and that it is a prototype of the stretching and folding dynamics that leads to deterministic chaos. It is generic in the sense that it can exhibit arbitrarily complicated symbolic dynamics and mixtures of hyperbolic and non–hyperbolic behaviors. Its construction was motivated by the best known early example of 'deterministic chaos', the Lorenz equation [1], see ref. [1] and remark 2.2.

Y. Pomeau's studies of the Lorenz attractor on an analog computer, and his insights into its stretching and folding dynamics motivated Hénon [2] to introduce the Hénon map in 1976. Hénon's and Lorenz's original papers can be found in reprint collections refs. [3, 4]. They are a pleasure to read, and are still the best introduction to the physics motivating such models. A detailed description of the dynamics of the Hénon map is given by Mira and coworkers [8], as well as very many other authors.

The Lozi map [10] is particularly convenient in investigating the symbolic dynamics of 2-*d* mappings. Both the Lorenz and Lozi systems are uniformly smooth systems with singularities. The continuity of measure for the Lozi map was proven by M. Misiurewicz [11], and the existence of the SRB measure was established by L.-S. Young.

[section 14.1]

Remark 3.3 Grasshoppers *vs.* butterflies. The 'sensitivity to initial conditions' was discussed by Maxwell, 30 years later by Poincaré. In weather prediction, the Lorentz' 'Butterfly Effect' started its journey in 1898, as a 'Grasshopper Effect' in a book review by W. S. Franklin [1]. In 1963 Lorenz ascribed a 'seagull effect' to an unnamed meteorologist, and in 1972 he repackaged it as the 'Butterfly Effect'.

Exercises

3.1. **<u>Poincaré sections of the Rössler flow.</u>**
(continuation of exercise 2.8) Calculate numerically a Poincaré section (or several Poincaré sections) of the Rössler flow. As the Rössler flow state space is $3D$, the flow maps onto a $2D$ Poincaré section. Do you see that in your numerical results? How good an approximation would a replacement of the return map for this section by a 1-dimensional map be? More precisely, estimate the thickness of the strange attractor. (continued as exercise 4.4)

(R. Paškauskas)

3.2. **A return Poincaré map for the Rössler flow.**
(continuation of exercise 3.1) That Poincaré return maps of figure 3.6 appear multimodal and non-invertible is an artifact of projections of a 2-dimensional return map $(R_n, z_n) \rightarrow (R_{n+1}, z_{n+1})$ onto a 1-dimensional subspace $R_n \rightarrow R_{n+1}$.

Construct a genuine $s_{n+1} = f(s_n)$ return map by parametrazing points on a Poincaré section of the attractor figure 3.5 by a Euclidean length s computed curvilinearly along the attractor section.

This is best done (using methods to be developed in what follows) by a continuation of the unstable manifold of the 1-cycle embedded in the strange attractor, figure 12.1 (b). (P. Cvitanović)

3.3. **Arbitrary Poincaré sections.** We will generalize the construction of Poincaré sections so that they can have any shape, as specified by the equation $U(x) = 0$.

(a) Start by modifying your integrator so that you can change the coordinates once you get near the Poincaré section. You can do this easily by writing the equations as

$$\frac{dx_k}{ds} = \kappa f_k, \qquad (3.22)$$

with $dt/ds = \kappa$, and choosing κ to be 1 or $1/f_1$. This allows one to switch between t and x_1 as the integration 'time.'

(b) Introduce an extra dimension x_{n+1} into your system and set

$$x_{n+1} = U(x). \qquad (3.23)$$

How can this be used to find a Poincaré section?

3.4. **Classical collinear helium dynamics.**
(continuation of exercise 2.10) Make a Poincaré surface of section by plotting (r_1, p_1) whenever $r_2 = 0$: Note that for $r_2 = 0$, p_2 is already determined by (7.6). Compare your results with figure 6.3 (b).

(Gregor Tanner, Per Rosenqvist)

3.5. **Hénon map fixed points.** Show that the two fixed points (x_0, x_0), (x_1, x_1) of the Hénon map (3.18) are given by

$$x_0 = \frac{-(1 - b) - \sqrt{(1 - b)^2 + 4a}}{2a},$$

$$x_1 = \frac{-(1 - b) + \sqrt{(1 - b)^2 + 4a}}{2a}.$$

3.6. **<u>How strange is the Hénon attractor?</u>**

(a) Iterate numerically some 100,000 times or so the Hénon map

$$\begin{bmatrix} x' \\ y' \end{bmatrix} = \begin{bmatrix} 1 - ax^2 + y \\ bx \end{bmatrix}$$

for $a = 1.4$, $b = 0.3$. Would you describe the result as a 'strange attractor'? Why?

(b) Now check how robust the Hénon attractor is by iterating a slightly different Hénon map, with $a = 1.39945219$, $b = 0.3$. Keep at it until the 'strange' attractor vanishes like the smile of the Chesire cat. What replaces it? Would you describe the result as a 'strange attractor'? Do you still have confidence in your own claim for the part (a) of this exercise?

3.7. **Fixed points of maps.** A continuous function F is a contraction of the unit interval if it maps the interval inside itself.

(a) Use the continuity of F to show that a 1-dimensional contraction F of the interval $[0, 1]$ has at least one fixed point.

(b) In a uniform (hyperbolic) contraction the slope of F is always smaller than one, $|F'| < 1$. Is the composition of uniform contractions a contraction? Is it uniform?